JOURNAL OF CATALYSIS 32, 148–154 (1974)

Infrared Spectra of Adsorbed Propyne*

D. M. SMITH†
Department of Chemistry, University of Denver, Denver, Colorado 80210

AND

J. R. BRAINARD, M. E. GRANT, AND C. A. LIEDER
Department of Chemistry, Hope College, Holland, Michigan 49423

Received September 7, 1973

Infrared spectra of propyne adsorbed on a series of SiO_2-supported metal chlorides have been obtained to delineate the effect of the electronic structure of the metal on the chemisorption previously described as a μ- and π-bonded surface complex. Data from a SiO_2-supported $MeCl_2$ series where Me is Ca, Cr, Mn, Fe, Co, Ni, Cu, and Zn, as well as from a SiO_2-supported $MeCl_3$ series where Me is Sc, Ga, Cr, and Fe, have been interpreted in terms of a ligand field model proposed for nitrosyl and carbonyl complexes. Shifts of ν_1, the $\equiv$C—H vibrational frequency, and ν_3, the —C$\equiv$C— vibrational frequency, from the corresponding frequencies of the gas phase molecule, are a function of metal *d*-orbital population. There is general agreement between the experimental data and the ligand field model of a distorted octahedral structure for the surface metal species. In the case of propyne adsorbed on Me(II) species, the infrared data are in agreement with a weak ligand field; for adsorption on Me(III) species, a strong ligand field is indicated.

INTRODUCTION

In a preliminary study of SiO_2-supported metal chloride catalysts for the vapor phase hydrochlorination of acetylene (*1*), infrared spectra of adsorbed acetylene and propyne indicated that the principal mode of adsorption is of the type

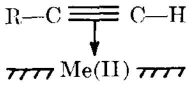

$$\begin{array}{c} R{-}C\equiv C{-}H \\ \downarrow \\ \mathrm{Me(II)} \end{array}$$

where R is H and CH_3, and Me is Ca, Mn, Zn, and Cu. This parallel-bonded surface species, where the alkyne–metal bond is a combination of μ- and π-bonding (*2*), is common to all of the SiO_2-supported metal chlorides investigated. Spectral data from propyne adsorption were most definitive. Shifts of ν_1, the $\equiv$C—H vibrational frequency, and ν_3, the —C$\equiv$C— vibrational frequency, from the corresponding frequencies of the gas phase molecule, correlated with the electron affinities of the metal ions but not with their ionization potentials. From this evidence, it was suggested that the μ-bonding was the more effective of the two orbital overlaps, the *d*-orbital involvement being secondary.

Because of the limited number of catalyst materials examined and the experimental limitations which obtained, the earlier study yielded no fundamental information on the role of the electronic structure of the metal in the adsorption of alkyne molecules. If the mode of adsorption proposed for acetylene and propyne is correct, however, the π-bonding and therefore the *d*-orbital population of the metal must exert

---

* Presented before the Division of Petroleum Chemistry, American Chemical Society, and is printed by permission.

† To whom queries concerning this paper should be sent.

some effect. The extent of this effect is an important question. It is important to an understanding of the bonding in the surface complex as well as the surface environment of the active metals, and has implications for the mechanisms of heterogeneous catalysis. It is an experimental fact, for example, that the nature of the metal in SiO_2-supported metal chlorides substantially affects their catalytic activity for addition reactions of acetylene (*1*), and there is evidence (*3–6*) that intermediates in such reactions are metal–acetylene complexes. The present work was undertaken in an effort to delineate the role of the metal *d* electrons in the adsorption of propyne and, thereby, to refine the bonding model for the spectroscopically observable surface complex.

EXPERIMENTAL METHODS

Apparatus. A Perkin-Elmer 621 infrared spectrophotometer with extended sample area was used for all spectroscopic measurements. A portable vacuum system allowed reproducible positioning of the sample at the focal point of the beam in the sample area of the spectrophotometer. A reference beam attenuator was employed to maintain the pen recording between 10 and 90% in frequency regions of low transmittance.

The sample cell was designed after that of Slager (*7*) and was of the inverted T type. The body was quartz graded to Pyrex at the top where connection to the vacuum system was effected with a size 40 spherical joint with O-ring seal (*8*). The sample was suspended in a holder, fashioned from quartz rod, from a hook so oriented above the connection to the vacuum system that the sample could not twist out of the infrared beam. This portion of the vacuum system, a 10-in. long segment containing a Teflon stopcock, could be detached by means of a second spherical joint so that some samples could be mounted within a dry box for the initial exclusion of air. Two separate heater windings around the cell body were employed to produce a furnace capable of heating the sample areas of the evacuated cell at temperatures to 400°C. Aluminum flanges with screw-on couplings were used to hold NaCl or CaF_2 50 mm windows in place against Viton O-rings. A chromel–alumel thermocouple, sealed through the upper arm of the cell, was positioned near the surface of the sample for accurate temperature measurements.

The vacuum system, capable of dynamic vacua to 10^{-6} Torr, was greaseless in the sample and gas handling sections. Viton O-rings were used in all joints and stopcocks (Ace Glass No. 8194-05,10). Pressures were measured with a Norton 524 cold cathode gauge.

The entire experimental system has been pictured elsewhere (*9*).

Reagents and procedures. The purification of reagents and preparation of adsorbents, as well as procedures employed in obtaining spectra, have been previously described in detail (*1*). The entire preparation of SiO_2-supported $CrCl_2$, $FeCl_2$ and VCl_3 samples, from the preparation of solutions to the mounting of pellets in the cell was carried out in an N_2-flushed dry box. In this work, several individual experiments were carried out for each material with a resulting standard deviation of 3 cm^{-1} for the frequency measurement of all reported bands.

RESULTS

Infrared spectra of propyne adsorbed on a series of SiO_2-supported metal chlorides were obtained for all of the $MeCl_2$ and $MeCl_3$ materials that could be prepared from first row transition elements. The SiO_2-supported $MeCl_2$ materials ($MeCl_2$–SiO_2) where Me was Ca, Cr, Mn, Fe, Co, Ni, Cu, and Zn, and the $MeCl_3$ materials ($MeCl_3$–SiO_2) where Me was Sc, Ga, Cr, and Fe, were the adsorbents studied.

Figure 1 is the spectrum between 4000 and 2000 cm^{-1} of propyne adsorbed on $CaCl_2$–SiO_2. Four frequencies of propyne, appearing at 3285, 2950, 2111, and 1445 cm^{-1} (not shown), which roughly correspond to the four normal vibrations of gas phase propyne in the 4000–1400 cm^{-1} range are observed. While there are individual variations in relative band intensity and frequency and, in a few cases, other absorptions appear, this set of frequencies is

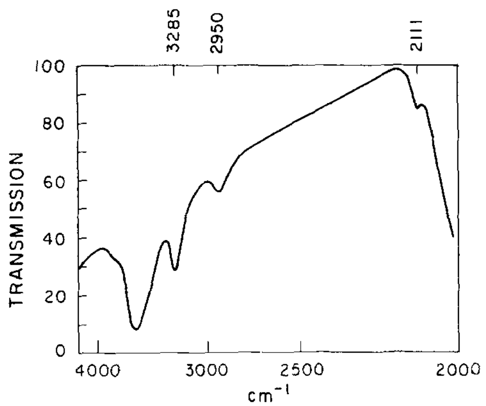

FIG. 1. Infrared spectrum of propyne adsorbed on SiO_2-supported $CaCl_2$.

common to all systems discussed below. That these spectra represent an essentially unchanged propyne molecule as the adsorbed species has been reported in earlier work (*1*). The bond between the propyne and the surface metal species has been described (*1*) in terms of a μ-bonded and π-bonded complex as shown in Fig. 2.

Analysis of the data is in terms of the frequency shifts, $\Delta\nu$, from the gas phase values exhibited by the ν_1 and ν_3 absorptions of propyne. The average ν_1 and ν_3 frequencies were 3340 and 2145 cm^{-1}, respectively, for gas phase propyne, and resulted from several measurements at varying pressures using the experimental cell.

$MeCl_2$–SiO_2. Results from the infrared spectra of propyne adsorbed on the $MeCl_2$–SiO_2 materials are plotted in Fig. 3 as $-\Delta\nu_1$ and $-\Delta\nu_3$ versus the *d*-orbital population for the metals. The shifts from the gas phase frequencies of ν_1 range from -55 cm^{-1} for Ca(d^0) to -117 cm^{-1} for Fe(d^6); shifts of ν_3 range from -33 cm^{-1} for Ca(d^0) to -180 cm^{-1} for Cu(d^9). Of particular interest in this plot are the low value for Mn(d^5), the maximum in $-\Delta\nu_1$ for Fe(d^6), and the high values of both $-\Delta\nu_1$ and $-\Delta\nu_3$ for Cu(d^9).

In experiments with $FeCl_2$–SiO_2 it was never possible to obtain a sufficiently well-resolved ν_3 absorption for an accurate calculation of $-\Delta\nu_3$. The reasons for this are presently unknown. In one preparation of $CoCl_2$–SiO_2 the adsorbed propyne yielded two sets of bands, one of which was attributed to a second type of surface site present in this case. (X-Ray patterns, run on all materials, showed a separate $CoCl_2$ phase present in this one; new preparations not exhibiting this phase revealed the usual infrared spectrum of adsorbed propyne.) Polymerization of the propyne was observed with all $NiCl_2$–SiO_2 samples, making the ν_1 and ν_3 absorptions difficult to measure accurately in some cases. Two types of adsorption are observed on $CuCl_2$–SiO_2 and have been ascribed (*1*) to the transformation of the μ- and π-bonded propyne to the species shown in Fig. 4.

Although the individual adsorption characteristics noted above were observed, the absorptions characteristic of the μ- and

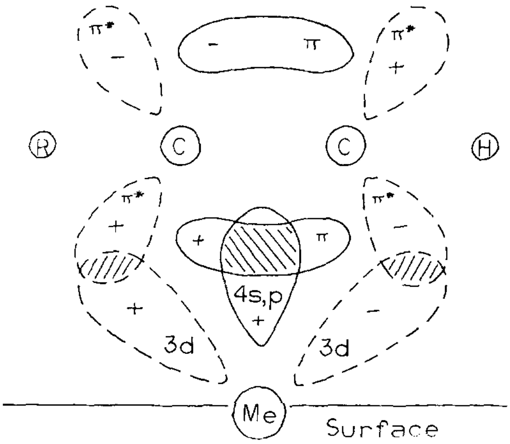

FIG. 2. A simplified representation of a μ- and π-bonded adsorbed alkyne.

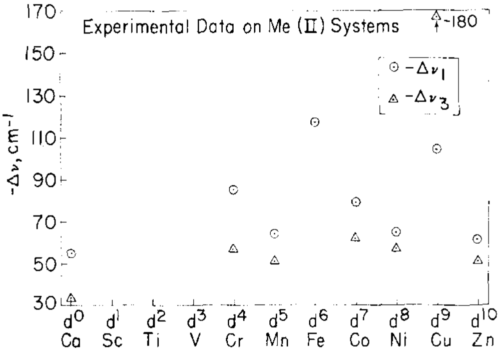

FIG. 3. Infrared frequency shifts from the gas phase values for propyne adsorbed on $MeCl_2$–SiO_2.

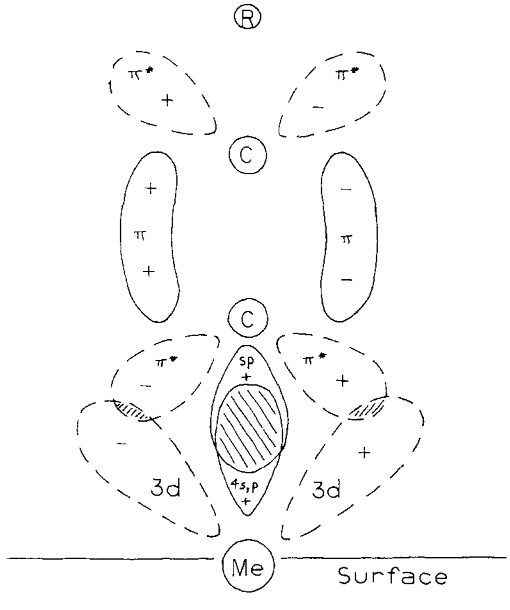

FIG. 4. A simplified representation of orbital interactions in the surface species R—C≡C—Me.

π-bonded propyne of Fig. 2 were common to all of the $MeCl_2$–SiO_2 materials studied. The data summarized in Fig. 3 represent that common behavior of the $MeCl_2$–SiO_2 materials in the adsorption of propyne.

$MeCl_3$–SiO_2. Results from the infrared spectra of propyne adsorbed on the $MeCl_3$–SiO_2 materials are summarized in Fig. 5. Against the *d*-orbital population of the metals are plotted $-\Delta\nu_1$ and $-\Delta\nu_3$. The shifts from the gas phase frequencies of ν_1 range from -61 cm^{-1} for Sc(d^0) to -85 cm^{-1} for Fe(d^5); shifts of ν_3 range from -42 cm^{-1} for Sc(d^0) to -57 cm^{-1} for Fe(d^5). Of particular interest in this plot is the maximum in both $-\Delta\nu_1$ and $-\Delta\nu_3$ for Fe(d^5).

It was not possible, in experiments with $GaCl_3$–SiO_2, to obtain a sufficiently well-resolved ν_3 absorption to accurately calculate a value for $-\Delta\nu_3$. As with $FeCl_2$–SiO_2, the reason for this adsorption behavior is presently unknown.

Although only four $MeCl_3$–SiO_2 materials were successfully prepared and examined spectroscopically, the spectrum (Fig. 1) characteristic of the μ- and π-bonded species (Fig. 2) is common to all.

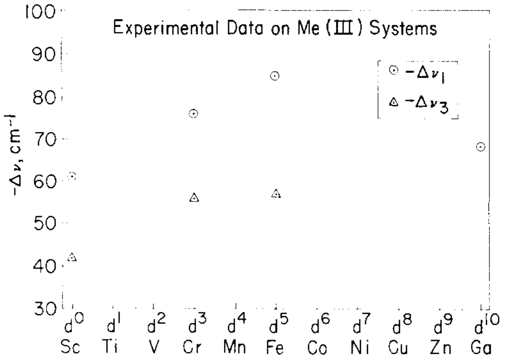

FIG. 5. Infrared frequency shifts from the gas phase values for propyne adsorbed on $MeCl_3$–SiO_2.

DISCUSSION

Data derived from the infrared spectra of adsorbed propyne, summarized in Figs. 3 and 5, have revealed a dependence of adsorption on the *d*-orbital population of the surface metal species. Interpretation of these results has been made in terms of a ligand field model adapted from one proposed by Gray, Bernal and Billig (*10*), for nitrosyls and carbonyls.

Although there is no detailed knowledge of the metal chloride surface species prior to propyne adsorption, the conditions of preparation and pretreatment of the $MeCl_{2-3}$–SiO_2 materials as well as the infrared spectra suggest $MeCl_{2-3}\cdot 3$–$2H_2O$ as the predominant species. Recent studies of Anderson (*11*, *12*) have indicated that the metal ions in SiO_2-supported Ni(II), Cu(II) and Cr(III) chlorides and nitrates occupy octahedral or distorted octahedral sites on the gel surface. Further, under such conditions as heat treatment, adsorption of NH_3 and varying methods by which the metal ion is introduced to the gel, the metal ions apparently remain in an octahedral environment where the coordinating ligands can be H_2O, anions, surface functional groups, or adsorbed molecules. While SiO_2-supported Co(II) occupies an octahedral site in gel freshly impregnated with $CoCl_2$, it appears to become tetrahedrally coordinated upon heat treatment or adsorption of NH_3; in $Co(NO_3)_2$-impregnated gel the Co(II) remains octahedral (*12*). While the preparation and pretreatment of the

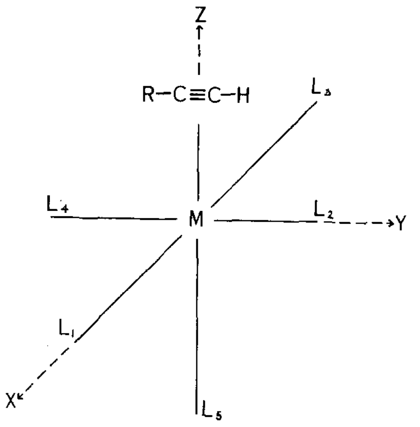

FIG. 6. The distorted octahedral structure for $MeL_5{\cdot}C_2HR$.

gels was not the same as those employed in this study, there is sufficient similarity in the materials to warrant the hypothesis that most of the metal species will be in an octahedral or distorted octahedral environment on the gel surface under the conditions of propyne chemisorption.

Considering the surface site as an MeL_5 species, with adsorbed alkyne serving as the sixth ligand in a distorted octahedral structure, then, the surface species after adsorption may be viewed as the complex $MeL_5{\cdot}C_2HR$ shown in Fig. 6. The molecular orbital scheme of Gray, Bernal and Billig (*10*), where NO or CO exert the predominant effect upon the ligand field, applicable to this case where the adsorbed propyne is such a ligand, is shown in Fig. 7.

This molecular orbital scheme can be used to consider the hypothetical stabilization of the surface species $MeL_5{\cdot}C_2HR$ and, therefore, to predict the pattern of frequency shifts which would be observed if this model were correct. Using a reasonable d-orbital splitting and the molecular orbital diagram of Fig. 7, it is possible to compute the stabilization energies of the surface complex, in units of the splitting factor Dq, for various d-orbital populations of the metal. Figures 8 and 9 show the resulting orbital diagrams and hypothetical stabilization energies in Dq and Dq′, respectively, for weak field and strong field cases. Figure 10 demonstrates the relative magnitudes of $-\Delta\nu$ (both $-\Delta\nu_1$ and $-\Delta\nu_3$) as a function of the d-orbital population of

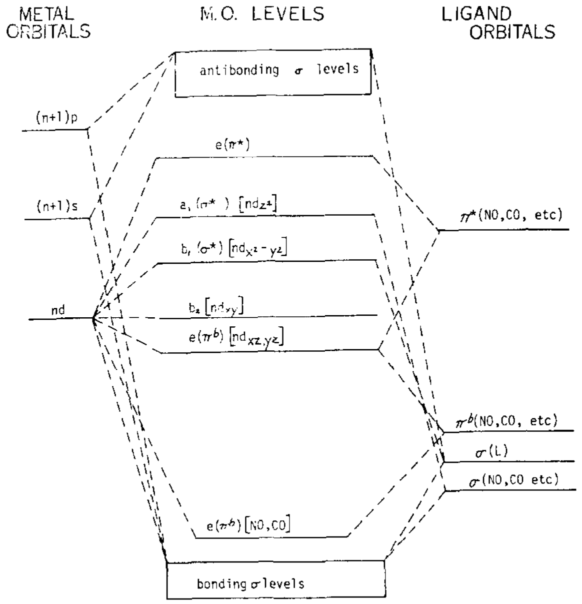

H.B. GRAY, I. BERNAL, E. BILLIG, J. AM. CHEM. SOC. 84. 3404 (1962).

FIG. 7. The molecular orbital energy level scheme for $MeL_5{\cdot}C_2HR$ (*10*).

Strong Field Stabilization Energies (in Dq') for

ML_5C_2HR

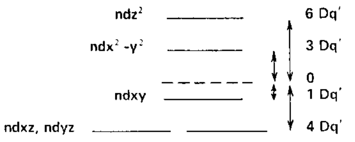

Configuration	S.E. in Dq'	Configuration	S.E. in Dq'
d^1	4	d^6	18
d^2	8	d^7	15
d^3	9 (or 12)	d^8	9 (or 12)
d^4	13 (or 16)	d^9	6
d^5	17	d^{10}	0

FIG. 8. Molecular orbital energy level scheme and weak field stabilization energies (in Dq) for $MeL_5 \cdot C_2HR$.

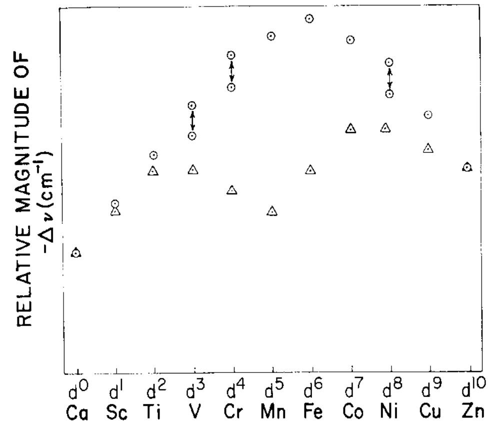

FIG. 10. Qualitative prediction of $-\Delta\nu$ resulting from propyne–metal interaction in a distorted octahedral environment. (△) Weak field case; (⊙) strong field case.

the metal species for weak field and strong field cases, respectively. The weak field case exhibits a minimum in $-\Delta\nu$ at d^5, accompanied by maxima at d^2, d^3 and d^7, d^8 together with a gradual increase from d^0 through d^{10}. The strong field case exhibits only one maximum, at d^6, with the usual gradual increase from d^0 through d^{10}. In plotting these dependences, a direct relationship between $-\Delta\nu$ and stabilization energy was assumed, and an arbitrary linear increase in $-\Delta\nu$ from d^0 to d^{10} was employed.

From Figs. 3 and 5 it can be observed that there is a general agreement between the experimental data and the ligand field model of a distorted octahedral structure for the surface metal species. In the case of propyne adsorbed on $MeCl_2$–SiO_2 species, Fig. 3, the infrared data are in agreement with a weak ligand field. For adsorption on $MeCl_3$–SiO_2 species, Fig. 5, the data are consistent with a strong ligand field. This is a reasonable result since the increased charge of the metal should result in a stronger splitting in the case of $MeCl_3$–SiO_2. While experimental data could not be obtained for some important members of these two series and individual variations make the plots deviate from the theoretical, it is felt that the general agreement with this model substantiates the nature of the chemisorbed state as the μ- and π-bonded species of Fig. 2. It also supports the evidence of Anderson (*11*, *12*) for the octahedral environment of certain metal ions at silica surfaces.

Weak Field Stabilization Energies (in Dq) for

ML_5C_2HR

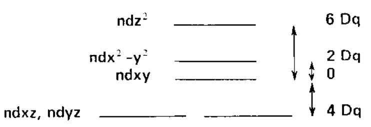

Configuration	S.E. in Dq	Configuration	S.E. in Dq
d^1	4	d^6	4
d^2	8	d^7	8
d^3	8	d^8	8
d^4	6	d^9	6
d^5	0	d^{10}	0

FIG. 9. Molecular orbital energy level scheme and strong field stabilization energies (in Dq') for $MeL_5 \cdot C_2HR$.

The extremely large shifts of $-\Delta\nu_1$ and $-\Delta\nu_3$ in the case of $CuCl_2$–SiO_2 must be rationalized. The $CuCl_2$–SiO_2 material was the only adsorbent to yield a reactive chemisorption (*1*), involving a change in the mode of adsorption from that pictured in Fig. 2 to that of Fig. 4, and is clearly unique among the $MeCl_2$–SiO_2 adsorbents studied. First of all, Cu(II) in ML_6 complexes undergoes strong Jahn-Teller distortion, a fact not considered in the preceding simple treatment. The magnitude of the additional stabilization energy could make the observed result reasonable. Secondly, the Cu(II) surface species may be of a different structural type with different orbital symmetry (i.e., tetrahedral rather than octahedral) as suggested by its apparent low activation energy for transformation into another species.

While the foregoing arguments are undoubtedly only an approximation of the actual nature of the adsorption phenomenon, the demonstration of the effect of *d*-orbital population on the adsorption and the interpretation in terms of a ligand field model of the surface complex appear to have defined the nature of the spectroscopically observable adsorbed state. It is hoped that this information will be useful in correlating the properties of the metal center with the catalytic properties of transition metal compounds toward heterogeneously catalyzed reactions of acetylenes.

ACKNOWLEDGMENTS

Acknowledgment is made to the donors of the Petroleum Research Fund, administered by the American Chemical Society, for support of this research. Initial financial support of Research Corporation and partial support by the National Science Foundation through an NSF-URP Grant to Hope College are also gratefully acknowledged. The authors are indebted to Drs. R. P. Eischens, R. G. Pearson, and T. L. Slager for encouragement and advice during this work.

REFERENCES

1. SMITH, D. M., WALSH, P. M., AND SLAGER, T. L., *J. Catal.* **11**, 113 (1968).
2. DEWAR, M. J. S., *Bull. Soc. Chim. Fr.* **18**, C71 (1951).
3. GEL'BSHTEIN, A. I., SILING, M. I., SERGEEVA, G. A., AND SHCHEGLOVA, G. G., *Kinet. Catal. (USSR)* **4**, 123 (1963).
4. GEL'BSHTEIN, A. I., AND SILING, M. I., *Kinet. Catal. (USSR)* **4**, 262 (1963).
5. GEL'BSHTEIN, A. I., SHCHEGLOVA, G. G., AND KHOMENKO, A. A., *Kinet. Catal. (USSR)* **4**, 543 (1963).
6. VASIL'EVA, I. B., GEL'BSHTEIN, A. I., TOLSTIKOVA, I. N., AND WANG-T'IONG, T., *Kinet. Catal. (USSR)* **5**, 119 (1964).
7. SLAGER, T. L., PhD dissertation, Carleton Univ., Ottawa, 1969.
8. DOTY, W. R., *Rev. Sci. Instrum.* **30**, 11 (1959).
9. SMITH, D. M., *Petrol. Res. Fund, Annu. Rep.* **15**, 237 (1970).
10. GRAY, H. B., BERNAL, I., AND BILLIG, E., *J. Amer. Chem. Soc.* **84**, 3404 (1962).
11. ANDERSON, J. H., *J. Catal.* **26**, 277 (1972).
12. ANDERSON, J. H., JR., *J. Catal.* **28**, 76 (1973).